

---

# Analytical and numerical study of the bifurcation of a cylindrical bar under uniaxial tension

Sabine Durand\* — Alain Combescure\*\*

\* CEA Saclay, DRN/DMT/SEMT/LM2S  
F-91191 Gif-sur-Yvette cedex

\*\* Laboratoire de Mécanique et Technologie, ENS de Cachan  
CNRS/Université Pierre et Marie Curie  
61 avenue du Président Wilson, F-94235 Cachan cedex

---

*ABSTRACT.* The influence of plasticity theory on the bifurcation of a cylindrical bar under large tensile strain is analyzed. A deformation theory of plasticity is assumed and the eigenvalue problem governing bifurcation is solved. A comparison is made between this solution and one obtained with a flow theory. The problem is then solved by means of the finite element method. Numerical computations are conducted for different geometries and material parameters and the results are compared with the analytical predictions.

*RÉSUMÉ.* L'influence de la théorie de plasticité adoptée pour la loi de comportement sur la bifurcation d'une barre cylindrique élasto-plastique incompressible soumise à de la traction est étudiée. La résolution analytique du problème aux valeurs propres gouvernant la bifurcation permet d'établir l'expression de la contrainte aux points de bifurcation obtenue pour une loi de déformation totale et de la comparer à celle obtenue pour une loi incrémentale. Ce même problème est ensuite résolu numériquement par la méthode des éléments finis. Les simulations numériques sont menées pour différentes géométries et différentes valeurs des caractéristiques du matériau.

*KEY WORDS :* bifurcation, uniqueness criterion, plasticity,  $J_2$  deformation theory, large strains.

*MOTS-CLÉS :* bifurcation, critère d'unicité, plasticité, loi de déformation totale, grandes déformations.

---

## 1. Introduction

When solids are subjected to tensile loading, necking instabilities can occur. A well-known example of this phenomenon is the necking of a cylindrical bar under uniaxial tension. This problem has already been extensively studied, both numerically and analytically. Within the body of work completed to date, various approaches have been adopted in order to predict the initiation of necking. To start necking, Norris *et al.* [NOR 78] used a geometry exhibiting an initial imperfection: the diameter of the bar's cross-section at its center was less than that at its extremities. The development of the neck is then simulated numerically through the use of finite differences.

Another approach consists of considering the onset of necking as a bifurcation from a uniform stress state. Such a perspective was adopted in the analytical study conducted by Hutchinson and Miles [HUT 74] as well as in the numerical study performed by Needleman [NEE 72]. These studies are based on Hill's [HIL 58] general theory of uniqueness and bifurcation. Hutchinson and Miles developed an exact expression for the true stress at bifurcation. The expression obtained reveals both that bifurcation always occurs after the maximum load has been reached and that the more slender is the bar, the nearer to the maximum load point bifurcation occurs. The same set of results have been yielded by Needleman's numerical study wherein the eigenvalue problem governing bifurcation is solved by means of the finite element method.

As opposed to the geometry used by Norris *et al.* in their computations, the authors consider a uniform bar. All of the studies cited above have employed a flow theory of plasticity. For structures subjected to compressive loading the buckling loads obtained with a deformation theory have often proved to be in closer agreement with experimental results than have the loads resulting from a flow theory (Batdorf [BAT 49], Bushnell [BUS 82]). We think that it is more reasonable to use the hypothesis of finite deformation theory for the computation of stress rate to predict bifurcation in case of tensile loads because, as in the compressive cases, it better takes into account the change in stress directions during the bifurcation. The resulting bifurcation loads should hence occur earlier than those obtained using flow theory. Our objective herein is to study the influence of the choice of plasticity theory adopted on the prediction of the initiation of necking in an incompressible elastic-plastic cylinder in tension. We shall use the approach developed in both Cheng *et al.* [CHE 71] and Hutchinson and Miles [HUT 74] in order to derive the expression for the true stress at bifurcation when a finite-strain version of deformation theory is considered. These analytical expressions will then be compared with the results obtained from the study of the bifurcation problem by means of the finite element method.

Sections 2 and 3 aim to present the uniqueness criterion and the constitutive laws, respectively. The equations governing the tension problem of a cylindrical bar are set forth in Section 4. The eigenvalue problem governing bifurcation is examined initially from an analytical perspective in Section 5, and then numerically in Section 6 by means of the finite element method.

## 2. Uniqueness criterion

Hill's [HIL 58] general theory of bifurcation of elastic-plastic solids provides the theoretical basis for our study. This section serves to recall the expression of the uniqueness criterion for a hypoelastic constitutive law of the form

$$\tau^J = \mathcal{H}(\tau) : \mathbf{D} \quad [1]$$

where  $\tau^J$  denotes the Jaumann derivative of the Kirchhoff stress tensor  $\tau$ ,  $\mathbf{D}$  the strain rate and  $\mathcal{H}$  a tensor exhibiting the following symmetry properties

$$\mathcal{H}_{ijkl} = \mathcal{H}_{jikl} = \mathcal{H}_{klij}$$

The current configuration has been taken as the reference configuration and the hypothesis that loading occurs everywhere in the plastic zone has been adopted. A sufficient condition for uniqueness of the rate problem can be written

$$\int_{\Omega} \frac{\partial w_i}{\partial x_j} \mathcal{K}_{ijkl} \frac{\partial w_k}{\partial x_l} d\Omega > 0 \quad \forall w / w = 0 \text{ on } S_u \quad [2]$$

with  $\mathbf{x}$  being the position vector of a material point in the current state and  $S_u$  representing the part of the boundary on which the displacement is being imposed. The tensors  $\mathcal{K}$  and  $\mathcal{H}$  are related by

$$\mathcal{K}_{ijkl} = \mathcal{H}_{ijkl} + \frac{1}{2}(\sigma_{jt}\delta_{ik} - \sigma_{jk}\delta_{it} - \sigma_{ik}\delta_{jl} - \sigma_{il}\delta_{jk})$$

The finite element discretisation of equation [2] leads to a classical zero eigenvalue and associated eigenmode research.

## 3. Constitutive equations

The material is assumed to be elastic-plastic, homogeneous and isotropic and hypoelastic models will be considered.

### 3.1. $J_2$ Flow theory

This large strain formulation of the Prandtl-Reuss equations has been proposed in both Hill [HIL 58] and McMeeking and Rice [MCM 75]. The constitutive equations

relate the Jaumann derivative of the Kirchhoff stress tensor to the strain rate. Elastic strains have been assumed to be small which enables us to state that the strain rate admits an additive decomposition into an elastic part  $\mathbf{D}^e$  and a plastic part  $\mathbf{D}^p$ .

For elastic loading or unloading, the constitutive law is given by

$$\tau_{ij}^J = \frac{E}{1+\nu} \left\{ \frac{\nu}{1-2\nu} D_{ll} \delta_{ij} + D_{ij} \right\} \quad [3]$$

where  $E$  and  $\nu$  denote Young's modulus and Poisson's ratio, respectively. For plastic loading, the constitutive equation is

$$\tau_{ij}^J = \frac{E}{1+\nu} \left\{ \frac{\nu}{1-2\nu} D_{ll} \delta_{ij} + D_{ij} \right\} - \frac{9E}{2[2(1+\nu)h + 3E]} \frac{\tau_{ij}^D \tau_{kl}^D}{\tau_{eq}^2} D_{kl} \quad [4]$$

with  $\tau^D$  and  $\tau_{eq}$  being defined by

$$\tau_{ij}^D = \tau_{ij} - \frac{1}{3} \tau_{ll} \delta_{ij} \quad \text{and} \quad \tau_{eq} = \left( \frac{3}{2} \tau_{ij}^D \tau_{ij}^D \right)^{\frac{1}{2}}$$

The value of  $h$  can be identified from the uniaxial stress-strain curve  $(\tau, \varepsilon)$  which gives the Kirchhoff stress  $\tau$  as a function of the logarithmic strain  $\varepsilon$ .  $h$  is given by

$$h = \frac{d\tau}{d\varepsilon^p}$$

The interpretation of  $h$  is shown on figure 1. If the tangent modulus  $E_t$  is defined as the slope of the curve  $(\tau, \varepsilon)$ , then  $h$  is related to  $E_t$  by:  $E_t = Eh/(E+h)$ .

### 3.2. $J_2$ deformation theory

The finite-strain version of  $J_2$  deformation theory which we are using was developed by Rudnicki and Rice [RUD 75]. The plastic strain rate  $\mathbf{D}^p$  is written as

$$D_{ij}^p = \begin{cases} 0 & \text{if } f < 0 \\ \frac{3}{2h_1} (\tau_{ij}^J)^D + \frac{9}{4\tau_{eq}^2} \left( \frac{1}{h} - \frac{1}{h_1} \right) \tau_{ij}^D \tau_{kl}^D \tau_{kl}^J & \text{if } f = 0 \end{cases}$$

where  $f$  designates the von Mises yield condition and the constant  $h_1$  is defined by

$$h_1 = \frac{\tau}{\varepsilon^p}$$

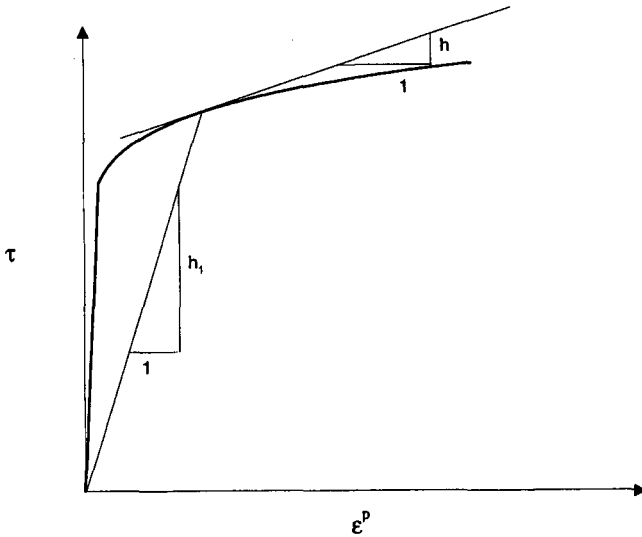


Figure 1. Interpretation of the coefficients  $h$  and  $h_1$

The elastic strain rate  $D^e$  remains given by the law

$$D_{ij}^e = \frac{1 + \nu}{E} \tau_{ij}^J - \frac{\nu}{E} \tau_{ll}^J \delta_{ij}$$

The relation between strain rates and stress rates in the plastic zone is

$$D_{ij} = \left( \frac{1 + \nu}{E} + \frac{3}{2h_1} \right) \tau_{ij}^J - \left( \frac{\nu}{E} + \frac{1}{2h_1} \right) \tau_{ll}^J \delta_{ij} + \frac{9}{4\tau_{\sigma q}^2} \left( \frac{1}{h} - \frac{1}{h_1} \right) \tau_{ij}^D \tau_{kl}^D \tau_{kl}^J \quad [5]$$

This relation may be inverted in order to express equation [5] in the form [1]. By multiplying [5] by  $\tau_{ij}^D$ , we obtain

$$\tau_{ij}^D D_{ij} = \left( \frac{1 + \nu}{E} + \frac{3}{2h} \right) \tau_{ij}^D \tau_{ij}^J \quad [6]$$

Using this expression, the constitutive law can therefore be written as

$$\tau_{ij}^J = \begin{cases} \frac{E}{1+\nu} \left\{ \frac{\nu}{1-2\nu} D_{ll} \delta_{ij} + D_{ij} \right\} & \text{if } f < 0 \\ \frac{2h_1 E}{2h_1(1+\nu) + 3E} \left\{ D_{ij} + \frac{2h_1 \nu + E}{2h_1(1-2\nu)} D_{ll} \delta_{ij} \right\} \\ - \frac{9E^2}{\tau_{eq}^2} \frac{(h_1 - h)}{[2h_1(1+\nu) + 3E][2h(1+\nu) + 3E]} \tau_{ij}^D \tau_{kl}^D D_{kl} & \text{if } f = 0 \end{cases} \quad [7]$$

#### 4. Problem Formulation

In our analysis, the material is assumed to be incompressible. The boundary-value problem is the following: the ends of the bar are subjected to an axial displacement and are shear free.

The cylindrical coordinate system  $(r, \theta, z)$  is used with  $0 \leq r \leq R$  and  $0 \leq z \leq L$ ,  $R$  and  $L$  being the current radius and length of the cylinder, respectively (figure 2).

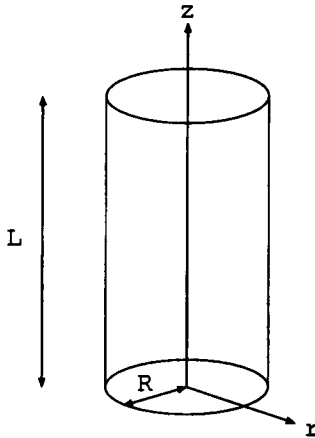


Figure 2. Geometry

The boundary conditions are as follows

$$\begin{cases} \text{for } r = R & \Pi_{rr} = \Pi_{\theta\theta} = \Pi_{zr} = 0 \\ \text{for } z = 0 & \Pi_{rz} = \Pi_{\theta z} = 0 \text{ and } u_z = -u_z^d \\ \text{for } z = L & \Pi_{rz} = \Pi_{\theta z} = 0 \text{ and } u_z = u_z^d \end{cases}$$

where  $\Pi$  represents the nominal stress tensor.

The constitutive laws were previously presented in Section 3 in the case of a compressible material. For an incompressible material, the Jacobian is equal to 1 and we have

$$\tau = \sigma \quad \text{and} \quad \dot{\tau} = \dot{\sigma}$$

The flow theory constitutive law becomes

$$\sigma_{ij}^J = \begin{cases} 2\mu D_{ij} + \frac{1}{3}\sigma_{il}^J \delta_{ij} & \text{if } f < 0 \text{ or } (f = 0 \text{ and } \dot{f} < 0) \\ 2\mu D_{ij} - \frac{9\mu^2}{h + 3\mu} \frac{\sigma_{ij}^D \sigma_{kl}^D}{\sigma_{eq}^2} D_{kl} + \frac{1}{3}\sigma_{il}^J \delta_{ij} & \text{if } (f = 0 \text{ and } \dot{f} = 0) \end{cases} \quad [8]$$

where  $\mu$  denotes the shear modulus and  $h = \frac{d\sigma}{d\varepsilon^p}$ .

For the deformation theory, [7] reduces to

$$\sigma_{ij}^J = \begin{cases} 2\mu D_{ij} + \frac{1}{3}\sigma_{il}^J \delta_{ij} & \text{if } f < 0 \\ \frac{2\mu h_1}{h_1 + 3\mu} D_{ij} - \frac{9\mu^2(h_1 - h)}{(h_1 + 3\mu)(h + 3\mu)} \frac{\sigma_{ij}^D \sigma_{kl}^D}{\sigma_{eq}^2} D_{kl} + \frac{1}{3}\sigma_{il}^J \delta_{ij} & \text{if } f = 0 \end{cases} \quad [9]$$

with:  $h_1 = \frac{\sigma}{\varepsilon^p}$ .

Equation [9.b] can be expressed in a form analogous to [8.b]

$$\sigma_{ij}^J = 2\mu_* D_{ij} - \frac{9\mu_*^2}{h_* + 3\mu_*} \frac{\sigma_{ij}^D \sigma_{kl}^D}{\sigma_{eq}^2} D_{kl} + \frac{1}{3}\sigma_{il}^J \delta_{ij}$$

with

$$\mu_* = \frac{\mu h_1}{h_1 + 3\mu} \quad \text{and} \quad \frac{1}{h_*} = \frac{1}{h} - \frac{1}{h_1}$$

### 5. Analytical Study of the Bifurcation Problem

The stress distribution in the bar remains a state of uniaxial and homogeneous stress up until a critical load at which bifurcation occurs. This bifurcation corresponds with the initiation of necking in the bar. An analytical study of this problem

has already been conducted by both Cheng *et al.* [CHE 71] and Hutchinson and Miles [HUT 74] for an incompressible elastic-plastic solid, in their analysis a flow theory of plasticity was assumed. The same approach has been employed herein but the deformation theory constitutive law [9] will be employed. In this section, the analytical study of the eigenvalue problem governing bifurcation is carried out in order to obtain an estimation of the bifurcation stress.

The deformation is assumed to be axisymmetric. Velocity fields are then of the form  $\mathbf{v} = (v_r(r, z), v_\theta = 0, v_z(r, z))$ .

The rate form of the equilibrium equations and of the boundary conditions governing the bifurcation problem are

$$\begin{cases} \frac{\partial \Delta \dot{\Pi}_{rr}}{\partial r} + \frac{\partial \Delta \dot{\Pi}_{rz}}{\partial z} + \frac{1}{r} (\Delta \dot{\Pi}_{rr} - \Delta \dot{\Pi}_{\theta\theta}) = 0 \\ \frac{\partial \Delta \dot{\Pi}_{zr}}{\partial r} + \frac{\partial \Delta \dot{\Pi}_{zz}}{\partial z} + \frac{\Delta \dot{\Pi}_{zr}}{r} = 0 \end{cases} \quad [10]$$

and

$$\begin{cases} \text{for } r = R \quad \Delta \dot{\Pi}_{rr} = \Delta \dot{\Pi}_{\theta r} = \Delta \dot{\Pi}_{zr} = 0 \\ \text{for } z = 0 \text{ and } z = L \quad \Delta \dot{\Pi}_{rz} = \Delta \dot{\Pi}_{\theta z} = 0 \quad \text{and} \quad \Delta v_z = 0 \end{cases}$$

where  $\Delta$  denotes the difference between a quantity associated with solution 2 and the same quantity associated with solution 1 :  $\Delta \mathbf{v} = \mathbf{v}^2 - \mathbf{v}^1$ ,  $\Delta \mathbf{\Pi} = \mathbf{\Pi}^2 - \mathbf{\Pi}^1$ .

The constitutive law can also be expressed in terms of the nominal stress-rate  $\dot{\mathbf{\Pi}}$ . By definition:

$$\begin{aligned} \dot{\mathbf{\Pi}} &= \dot{\boldsymbol{\sigma}} - \boldsymbol{\sigma} \mathbf{L}^T \\ &= \boldsymbol{\sigma}^J + \mathbf{W} \boldsymbol{\sigma} - \boldsymbol{\sigma} \mathbf{D} \end{aligned}$$

with  $\mathbf{L}$  and  $\mathbf{W}$  being the velocity gradient tensor and the rate of rotation tensor, respectively.

At bifurcation the stress distribution being uniaxial, let  $\sigma = \sigma_{zz}$  denotes the Cauchy stress.  $\dot{\mathbf{\Pi}}$  can then be written as

$$\left\{ \begin{array}{l} \dot{\Pi}_{rr} = \frac{2E_s}{3}D_{rr} + \frac{1}{3}(\beta_* + \sigma)D_{zz} + \dot{p} \\ \dot{\Pi}_{\theta\theta} = \frac{2}{3}E_sD_{\theta\theta} + \frac{1}{3}(\beta_* + \sigma)D_{zz} + \dot{p} \\ \dot{\Pi}_{zz} = \left[ \frac{2}{3}E_s - \frac{2}{3}(\beta_* + \sigma) \right] D_{zz} + \dot{p} \\ \dot{\Pi}_{rz} = \left( \frac{2}{3}E_s + \sigma \right) D_{rz} - \sigma \frac{\partial v_z}{\partial r} \\ \dot{\Pi}_{zr} = \left( \frac{2}{3}E_s - \sigma \right) D_{rz} \end{array} \right. \quad [11]$$

with the other components being zero.  $\dot{p}$  and  $\beta_*$  are defined by

$$\dot{p} = \frac{1}{3} \left( \dot{\Pi}_{rr} + \dot{\Pi}_{\theta\theta} + \dot{\Pi}_{zz} \right) \quad \text{and} \quad \beta_* = \frac{9\mu_*^2}{h_* + 3\mu_*} = \frac{9\mu^2(h_1 - h)}{(h_1 + 3\mu)(h + 3\mu)}$$

$h$  and  $h_1$  can be expressed as a function of both the tangent modulus  $E_t$  and the secant modulus  $E_s$  ( $E_s = \sigma/\varepsilon$ )

$$h = \frac{EE_t}{E - E_t} \quad \text{and} \quad h_1 = \frac{EE_s}{E - E_s}$$

the values of these moduli being given by the stress-strain curve. These relations leads to the following expressions for  $\mu_*$  and  $\beta_*$

$$\mu_* = \frac{E_s}{3} \quad \text{and} \quad \beta_* = E_s - E_t$$

The strain rate  $\mathbf{D}$  is related to the velocities by

$$D_{rr} = \frac{\partial v_r}{\partial r}, \quad D_{\theta\theta} = \frac{v_r}{r}, \quad D_{zz} = \frac{\partial v_z}{\partial z}, \quad D_{rz} = \frac{1}{2} \left( \frac{\partial v_r}{\partial z} + \frac{\partial v_z}{\partial r} \right) \quad \text{and} \quad D_{r\theta} = D_{\theta z} = 0$$

Using the constitutive equations [11] and the incompressibility condition  $tr\mathbf{D} = 0$ , the equilibrium equations [10] become

$$\left\{ \begin{array}{l} -\frac{1}{3} \left( E_t^c + \frac{\sigma_c}{2} \right) \frac{\partial^2 \Delta v_z}{\partial r \partial z} + \left( \frac{E_s^c}{3} + \frac{\sigma_c}{2} \right) \frac{\partial^2 \Delta v_r}{\partial z^2} + \frac{\partial \Delta \dot{p}}{\partial r} = 0 \\ \left( -\frac{E_s^c}{3} + \frac{2E_t^c}{3} - \frac{\sigma_c}{6} \right) \frac{\partial^2 \Delta v_z}{\partial z^2} + \frac{1}{r} \left( \frac{E_s^c}{3} - \frac{\sigma_c}{2} \right) \frac{\partial}{\partial r} \left( r \frac{\partial \Delta v_z}{\partial r} \right) + \frac{\partial \Delta \dot{p}}{\partial z} = 0 \end{array} \right.$$

where  $\sigma_c$ ,  $E_t^c$  and  $E_s^c$  are respectively, the values of the stress, the tangent modulus and the secant modulus at bifurcation.

By eliminating  $\Delta \dot{p}$  from these equations, we obtain

$$\left(\frac{E_s^c}{3} - \frac{\sigma_c}{2}\right) \frac{\partial}{\partial r} \left[ \frac{1}{r} \frac{\partial}{\partial r} \left( r \frac{\partial \Delta v_z}{\partial r} \right) \right] - \left(\frac{E_s^c}{3} - E_t^c\right) \frac{\partial^3 \Delta v_z}{\partial r \partial z^2} - \left(\frac{E_s^c}{3} + \frac{\sigma_c}{2}\right) \frac{\partial^3 \Delta v_r}{\partial z^3} = 0 \quad [12]$$

In order to describe the problem by a differential equation which only involves the variable  $r$ , we seek a solution of the form

$$\Delta v_r = -\frac{\partial \Phi}{\partial z}, \quad \Delta v_z = \frac{1}{r} \frac{\partial (r \Phi)}{\partial r}$$

with the function  $\Phi$  being defined by

$$\Phi(r, z) = \phi(r) \sin\left(\frac{k\pi z}{L}\right), \quad k = 1, 2, \dots$$

Equation [12] can thereby be reduced to the differential equation

$$(\mathcal{L}^2 + 2\gamma^2 b \mathcal{L} + \gamma^4 c) \phi = 0 \quad [13]$$

where

$$\gamma = \frac{k\pi R}{L}, \quad 2b = \frac{E_s^c/3 - E_t^c}{E_s^c/3 - \sigma_c/2}, \quad c = \frac{E_s^c/3 + \sigma_c/2}{E_s^c/3 - \sigma_c/2}$$

and

$$\mathcal{L} = \frac{\partial}{\partial \zeta} \left[ \frac{1}{\zeta} \frac{\partial}{\partial \zeta} (\zeta \cdot) \right] \quad \text{with} \quad \zeta = \frac{r}{R}$$

The boundary conditions for both  $z = 0$  and  $z = L$  are then identically satisfied, and the conditions on the lateral surface  $r = R$  ( $\zeta = 1$ ) become

$$\text{for } \zeta = 1 \quad \begin{cases} \mathcal{L}(\phi) + \gamma^2 \phi = 0 \\ \gamma^2 \delta_1 \frac{\partial}{\partial \zeta} (\zeta \phi) - \delta_2 \frac{\partial}{\partial \zeta} [\zeta \mathcal{L}(\phi)] + \gamma^2 \delta_3 \phi = 0 \end{cases} \quad [14]$$

with

$$\delta_1 = \sigma_c/2 - E_t^c, \delta_2 = \sigma_c/2 - E_s^c/3, \delta_3 = 2E_s^c/3$$

Equation [13] can also be rewritten as

$$(\mathcal{L} + \gamma^2 \rho_1^2) (\mathcal{L} + \gamma^2 \rho_2^2) \phi = 0 \tag{15}$$

If  $\Delta = b^2 - c > 0$ , the roots  $\rho_1^2$  and  $\rho_2^2$  are real and defined by

$$\rho_1^2 = b + \sqrt{b^2 - c} \quad \text{and} \quad \rho_2^2 = b - \sqrt{b^2 - c}$$

If  $\Delta < 0$ , the roots  $\rho_1^2$  and  $\rho_2^2$  are complex and

$$\rho_1^2 = b + i\sqrt{c - b^2} \quad \text{and} \quad \rho_2 = \bar{\rho}_1$$

The general solution to equation [15] is

$$\phi = A_1 J_1(\rho_1 \gamma \zeta) + A_2 J_1(\rho_2 \gamma \zeta)$$

where  $J_1$  is the Bessel function of the first kind. Since  $\phi$  should remain bounded for  $\zeta = 0$ , the Bessel functions of the second kind don't appear in the expression of  $\phi$ .

Substitution of this solution in the boundary conditions [14] leads to the following condition for bifurcation

$$\begin{aligned} & (1 - \rho_1^2) J_1(\rho_1 \gamma) [\rho_2 \gamma (\delta_1 + \rho_2^2 \delta_2) J_0(\rho_2 \gamma) + \delta_3 J_1(\rho_2 \gamma)] \\ & - (1 - \rho_2^2) J_1(\rho_2 \gamma) [\rho_1 \gamma (\delta_1 + \rho_1^2 \delta_2) J_0(\rho_1 \gamma) + \delta_3 J_1(\rho_1 \gamma)] = 0 \end{aligned} \tag{16}$$

The quantity  $\gamma$ , i.e. the ratio  $R/L$ , is assumed to be small. Thus the Bessel functions may be approximated using the series representation to order  $(\rho_1 \gamma)^6$  and  $(\rho_2 \gamma)^6$ . If  $\Delta > 0$ , equation [16] then becomes

$$\begin{aligned} & \frac{1}{2} \gamma^2 (b^2 - c)^{\frac{1}{2}} \rho_1 \rho_2 \left\{ \left[ \delta_1 + \delta_2 + \frac{1}{2} \delta_3 \right] - \frac{\gamma^2}{8} [\delta_1 (1 + 2b) + \delta_2 (4b - c) + b \delta_3] \right. \\ & \left. + \frac{\gamma^4}{192} \left[ 2\delta_1 (3b + c) + 2\delta_2 (3b - c + 2cb^2) + \delta_3 \left( \frac{1}{2} c + b \right) \right] \right\} = 0 \end{aligned} \tag{17}$$

If  $\Delta < 0$ , equation [16] reduces to

$$\frac{1}{2}\gamma^2(c - b^2)^{\frac{1}{2}}|\rho|^2 \left\{ \left[ \delta_1 + \delta_2 + \frac{1}{2}\delta_3 \right] - \frac{\gamma^2}{8} [\delta_1(1 + 2b) + \delta_2(4b - c) + b\delta_3] + \frac{\gamma^4}{192} \left[ 2\delta_1(c + 2b + 2b^2) + 2\delta_2(c - 2cb + 6b^2) + \frac{1}{2}\delta_3(c + 4b^2) \right] \right\} = 0 \quad [18]$$

The coefficients of the constant term and of the term of order  $\gamma^2$  of these two equations can be expressed as follows

$$\delta_1 + \delta_2 + \frac{1}{2}\delta_3 = \sigma_c - E_t^c \quad [19]$$

$$\delta_1(1 + 2b) + \delta_2(4b - c) + b\delta_3 = \frac{\frac{2}{3}\sigma_c E_s^c - \frac{\sigma_c^2}{2} + E_t^{c2} - \sigma_c E_t^c - \frac{E_s^c E_t^c}{3}}{\frac{E_s^c}{3} - \frac{\sigma_c}{2}} \quad [20]$$

The term [20] is of order  $O(\sigma_c, E_t^c, E_s^c)$ . Since  $\gamma$  is assumed to be small, the terms  $\gamma^4 \times O(\sigma_c, E_t^c, E_s^c)$  are neglected. Regardless of the sign of  $\Delta$ , equations [17] and [18] both reduce to

$$(\sigma_c - E_t^c) \left( \frac{E_s^c}{3} - \frac{\sigma_c}{2} \right) - \frac{\gamma^2}{8} \left[ \frac{2}{3}\sigma_c E_s^c - \frac{\sigma_c^2}{2} + E_t^{c2} - \sigma_c E_t^c - \frac{E_s^c E_t^c}{3} \right] = 0 \quad [21]$$

The coefficients of equation [21] are therefore functions of the unknown quantities  $E_s^c$  and  $E_t^c$ . The value of  $E_t^c$  is approximated using expansion about the maximum load point

$$E_t(\sigma_c) = E_t(\sigma_m) + (\sigma_c - \sigma_m) \frac{dE_t}{d\sigma}(\sigma_m)$$

whith  $\sigma_m$  being the stress at the maximum load point. At that point, the stress is equal to the tangent modulus

$$\sigma_m = E_t^m \quad [22]$$

Using [22], we obtain

$$E_t^c = \sigma_m + (\sigma_c - \sigma_m) \left. \frac{dE_t}{d\sigma} \right|_m \quad [23]$$

The secant modulus at bifurcation  $E_s^c$  is also expanded about the maximum load point

$$E_s(\sigma_c) = E_s(\sigma_m) + (\sigma_c - \sigma_m) \frac{dE_s}{d\sigma}(\sigma_m)$$

From the definition of the secant modulus

$$E_s = \frac{\sigma}{\varepsilon}$$

it follows that

$$\frac{dE_s}{d\sigma} = \frac{1}{\varepsilon} - \frac{\sigma}{\varepsilon^2} \frac{d\varepsilon}{d\sigma} = \frac{1}{\varepsilon} \left( 1 - \frac{E_s}{E_t} \right)$$

Hence,  $E_s^c$  can be expressed as a function of  $E_t^m$  and  $E_s^m = E_s(\sigma_m)$

$$E_s^c = E_s^m + \frac{E_s^m}{\sigma_m} \left( 1 - \frac{E_s^m}{E_t^m} \right) (\sigma_c - \sigma_m) \quad [24]$$

With terms of order  $(\sigma_c - \sigma_m)^2$  neglected, the expressions of the coefficients of equation [21] are

$$(\sigma_c - E_t^c) \left( \frac{E_s^c}{3} - \frac{\sigma_c}{2} \right) = (\sigma_c - \sigma_m) \left( \frac{1}{3} E_s^m - \frac{1}{2} \sigma_m \right) \left( 1 - \left. \frac{dE_t}{d\sigma} \right|_m \right)$$

and

$$\begin{aligned} & \frac{2}{3} \sigma_c E_s^c - \frac{\sigma_c^2}{2} + E_t^{c2} - \sigma_c E_t^c - \frac{E_s^c E_t^c}{3} = \\ & \sigma_m \left( \frac{1}{3} E_s^m - \frac{1}{2} \sigma_m \right) + (\sigma_c - \sigma_m) \left[ E_s^m - \frac{1}{3} \frac{E_s^{m2}}{\sigma_m} - 2\sigma_m + \left( \sigma_m - \frac{E_s^m}{3} \right) \left. \frac{dE_t}{d\sigma} \right|_m \right] \end{aligned}$$

which leads to the following value of  $\sigma_c$

$$\sigma_c = \sigma_m + \left(1 - \frac{dE_t}{d\sigma} \Big|_m\right)^{-1} \frac{\gamma^2}{8} \sigma_m \quad [25]$$

Hutchinson and Miles have established that in the case of the flow theory constitutive law [8]  $\sigma_c$  is given by

$$\sigma_c = \sigma_m + \left(1 - \frac{dE_t}{d\sigma} \Big|_m\right)^{-1} \left(\frac{\gamma^2}{8} \sigma_m + \frac{\gamma^4}{192} \mu\right) \quad [26]$$

In [25], terms of order  $O(\gamma^4 \sigma_c, \gamma^4 E_t^c, \gamma^4 E_s^c)$  have been neglected while equation [26] include terms of order  $\gamma^4 E$ . It is important to note that the expression obtained by Hutchinson and Miles rests on the assumption that  $E_t^c \ll E$ . In our study we assume that  $E_s^c \ll E$ . This hypothesis allows us to compare the results predicted by both plasticity theories.

Both theories predict that bifurcation occurs after the maximum load point. The value of the stress at bifurcation depends on the elastic-plastic properties of the material and on the ratio radius to length  $R/L$  of the cylinder. For small values of  $R/L$ , i.e. for slender bars, bifurcation occurs shortly after the maximum load point. The critical stress predicted by the flow theory is always greater than the stress predicted by the deformation theory.

## 6. Numerical results

In this section, the eigenvalue problem governing bifurcation is solved numerically by means of the finite element method. The bifurcation loads are characterized by the variational equation

$$\int_{\Omega} \frac{\partial w_i}{\partial x_j} \mathcal{K}_{ijkl} \frac{\partial w_k}{\partial x_l} d\Omega = 0 \quad \forall w / w = 0 \text{ on } S_u$$

In terms of finite elements, determining the displacement  $u_c^d$  at which bifurcation occurs reduces to solving the equation

$$K(u_c^d) w = 0$$

where  $K$  represents the global stiffness matrix and  $w$  the vector of nodal velocities.

An incremental calculation is first performed which enables to determinate the state of the system at each time step (stress distribution, displacements, strain-hardening

variable). The stiffness matrix is then evaluated at each time step and the eigenvalue problem is solved in order to obtain the value of  $u_c^d$  for which the matrix  $K$  becomes singular.

Computations were conducted both for a material whose stress-strain curve is bilinear (where the tangent modulus  $E_t$  remains constant) and for a material whose stress-strain curve is represented by a piecewise power law (where the tangent modulus depends on  $\sigma$ ). The computations have been carried out using the finite element code Castem 2000 in which the global stiffness matrix corresponding to the flow theory constitutive law [3,4] and the matrix corresponding to the deformation theory law [7] have been added. These numerical results are then compared with the analytical expressions derived in the previous section.

### 6.1. Bilinear hardening law

The elastic-plastic properties of the material are specified by the parameters  $E = 2.10^5$  MPa,  $\nu = 0.499$ ,  $E_t = 450$  MPa and the yield stress  $\sigma_y$  is 400 MPa. The computations were carried out for three different geometries: the initial length is  $L_0 = 55$  mm and three values of the radius are considered:  $R_0 = 5$  mm,  $R_0 = 3.75$  mm and  $R_0 = 2.5$  mm. The meshes of the three cylinders are shown in figure 3. The elements used are 9-node quadrilaterals. The hypothesis of axisymmetric deformation has been used in the numerical analysis.

The solution obtained by the finite element calculation is the fundamental solution: the stress distribution in the cylinder remains uniaxial and homogeneous throughout the entire loading.

For a constant tangent modulus, the expression of  $\sigma_c$  is given by

$$\sigma_c = \sigma_m + \frac{\gamma^2}{8} \sigma_m + \frac{\gamma^4}{192} \frac{E}{3}$$

in the case of the  $J_2$  flow theory and by

$$\sigma_c = \sigma_m + \frac{\gamma^2}{8} \sigma_m$$

in the case of the  $J_2$  deformation theory.

$\gamma$  is approximated by replacing  $R$  and  $L$ , the radius and length at bifurcation, by  $R_m$  and  $L_m$  the radius and length at maximum load

$$\gamma \simeq \gamma_m = \frac{k\pi R_m}{L_m}$$

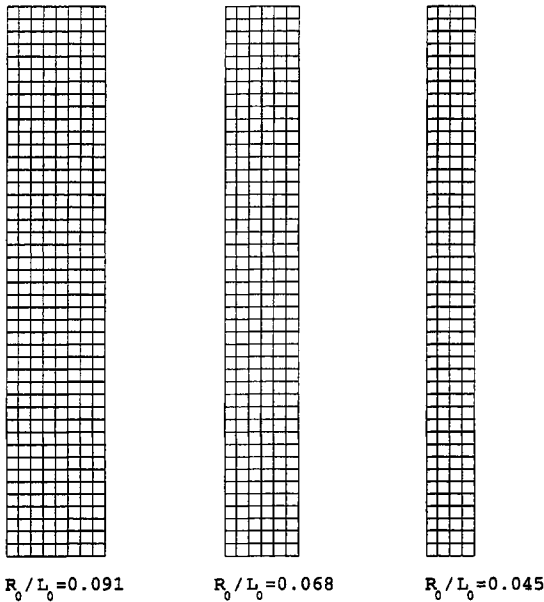


**Figure 3.** Meshes used for the F.E. computations

Since the tangent modulus  $E_t$  is constant,  $L_m$  and  $R_m$  are given by

$$L_m = L_0 \exp \left[ 1 + \sigma_y \left( \frac{1}{E} - \frac{1}{E_t} \right) \right] \quad \text{and} \quad R_m = \frac{R_0}{\left\{ \exp \left[ 1 + \sigma_y \left( \frac{1}{E} - \frac{1}{E_t} \right) \right] \right\}^{\frac{1}{2}}}$$

For the material properties chosen, the following values are obtained:  $\sigma_m = 450$  MPa,  $L_m = 61.587$  mm,  $u_d^m = 3.293$  mm.

The lowest bifurcation point is obtained for  $k = 1$ . This mode is not symmetric: necking occurs at one end of the bar. The second bifurcation mode ( $k = 2$ ) is a symmetric one and necking is located at the middle of the bar. If the numerical study of bifurcation is carried out by considering only half of the cylinder then only symmetric modes are found and the lowest bifurcation value obtained corresponds with  $k = 2$ .

The values of the stress  $\sigma_c$  and of the prescribed axial displacement  $u_c^d$  for the two lowest bifurcation modes ( $k = 1$  and  $k = 2$ ) obtained with both theories of plasticity are presented in figure 4. This table enables comparing the values resulting from the analytical formulae and the numerical computations for the three values of the ratio of radius to length:  $R_0/L_0=0.091$ ,  $R_0/L_0=0.068$  and  $R_0/L_0=0.045$ .

These results reveal that the values of  $\sigma_c$  given by the analytical formulae are in good agreement with those obtained by the finite element computation. The bifurcation stress  $\sigma_c$  obtained with the flow theory is always greater than that obtained with

		k = 1			k = 2		
		$u_c^d$	$\sigma_c$	$\sigma_c$	$u_c^d$	$\sigma_c$	$\sigma_c$
		numerical	analytical	numerical	analytical	numerical	analytical
$R_0/L_0 = 0.091$	deformation theory	3.52	453.300	453.281	4.17	462.632	463.124
	flow theory	3.60	454.460	454.462	5.11	475.794	482.025
$R_0/L_0 = 0.068$	deformation theory	3.42	451.847	451.845	3.80	457.344	457.382
	flow theory	3.45	452.284	452.219	4.16	462.490	463.363
$R_0/L_0 = 0.045$	deformation theory	3.35	450.827	450.820	3.52	453.300	453.281
	flow theory	3.36	450.973	450.894	3.61	454.604	454.462

**Figure 4.** Numerical and analytical values of  $u_c^d$  and  $\sigma_c$  at the two lowest bifurcation modes ( $E_t = 450$  MPa)

the deformation theory; moreover, this difference grows as the cylinder's thickness increases.

The more slender the cylinder, i.e the smaller  $\gamma$  is, the nearer to the maximum load bifurcation occurs, as for example for the ratio  $R_0/L_0=0.045$ . Furthermore, the first and second bifurcation points are then closer. The stress values for the second bifurcation mode in the case  $R_0/L_0=0.091$  are those displaying the greatest discrepancy between the analytical solution and the numerical solution, which can be explained by the fact that in this case  $\gamma$  is not small in comparison with 1 ( $\gamma_m = 0.483$ ). For the selected value of the tangent modulus for these computations ( $E_t = 450$  MPa), bifurcation occurs for relatively small strains (between 12% and 18%).

Figure 5 presents the results obtained for  $E_t = 1300$  MPa; in that case bifurcation occurs for strains of the order of 100%. The conclusions stated within the framework of the computations conducted with  $E_t = 450$  MPa remain valid.

		k = 1			k = 2		
		$u_c^d$	$\sigma_c$	$\sigma_c$	$u_c^d$	$\sigma_c$	$\sigma_c$
		numerical	analytical	numerical	analytical	numerical	analytical
$R_0/L_0 = 0.091$	deformation theory	27.635	1301.675	1301.658	27.845	1306.617	1306.631
	flow theory	27.640	1301.793	1301.694	27.875	1307.321	1307.209
$R_0/L_0 = 0.045$	deformation theory	27.585	1300.495	1300.414	27.635	1301.67	1301.658
	flow theory	27.585	1300.495	1300.417	27.640	1301.792	1301.694

**Figure 5.** Numerical and analytical values of  $u_c^d$  and  $\sigma_c$  at the two lowest bifurcation modes ( $E_t = 1300$  MPa)

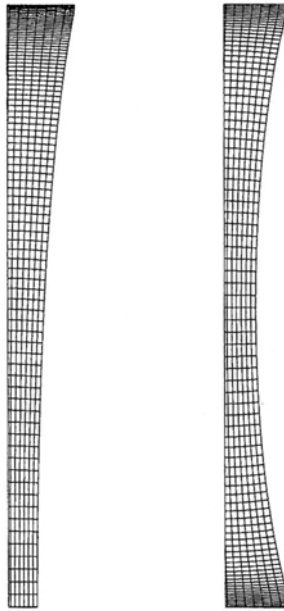


**Figure 6.** *Bifurcation modes*

**6.2. Power hardening law**

In this section, the tangent modulus  $E_t$  is variable and the stress-strain curve is defined by the following relations

$$\left\{ \begin{array}{ll} \sigma = E\varepsilon & \text{for } \sigma < \sigma_y \\ \sigma = \sigma_y^{(n-1)/n} (E\varepsilon)^{1/n} & \text{for } \sigma \geq \sigma_y \end{array} \right. \quad [27]$$

Calculations have been carried out for three values of  $n$ : 2, 5 and 10. The same values are retained for  $E$ ,  $\nu$  and  $\sigma_y$  and three values of the radius are considered:  $R_0 = 3.75$  mm,  $R_0 = 2.5$  mm and  $R_0 = 1$  mm, with the length remaining  $L_0 = 55$  mm.

In order to calculate the value of  $\sigma_c$ , we need to derive the expression of  $\gamma_m$ ,  $\sigma_m$  and  $dE_t/d\sigma(\sigma_m)$  when the uniaxial law [27] is considered.

The tangent modulus can then be expressed as a function of  $\sigma$

$$E_t = \frac{E}{n} \left( \frac{\sigma}{\sigma_y} \right)^{1-n}$$

Using the relation  $\sigma_m = E_t^m$ , we obtain

$$\sigma_m = \left(\frac{E}{n}\right)^{1/n} \sigma_y^{(n-1)/n}$$

and

$$\left.\frac{dE_t}{d\sigma}\right|_m = 1 - n$$

The strain at maximum load is given by  $\epsilon_m = 1/n$  and the length and the radius can be written as

$$L_m = L_0 \exp\left(\frac{1}{n}\right) \quad \text{and} \quad R_m = \frac{R_0}{\left[\exp\left(\frac{1}{n}\right)\right]^{\frac{1}{2}}}$$

Figures 7, 8 and 9 display the results obtained for  $n = 2, 5$  and  $10$ , respectively.

Here again a very good agreement between numerical and analytical results can be observed. The analytical bifurcation stress obtained for both plasticity theories are so close that the numerical results cannot grasp the difference. The difference between the two theories is larger when the cylinder is thick and when the value of  $n$  is high. For all these computations the first and second bifurcation modes appear to be very close.

		$k = 1$			$k = 2$		
		$u_c^d$	$\sigma_c$	$\sigma_c$	$u_c^d$	$\sigma_c$	$\sigma_c$
		numerical	analytical	analytical	numerical	analytical	analytical
$R_0/L_0 = 0.068$	deformation theory	17.868	6328.456	6328.602	17.959	6341.107	6340.742
	flow theory	17.868	6328.456	6328.620	17.959	6341.107	6341.033
$R_0/L_0 = 0.045$	deformation theory	17.853	6326.365	6326.354	17.894	6332.076	6331.750
	flow theory	17.853	6326.365	6326.357	17.895	6332.215	6331.807
$R_0/L_0 = 0.018$	deformation theory	17.841	6324.692	6324.843	17.850	6325.947	6325.706
	flow theory	17.841	6324.692	6324.843	17.850	6325.947	6325.708

**Figure 7.** Numerical and analytical values of  $u_c^d$  and  $\sigma_c$  at the two lowest bifurcation modes ( $n = 2$ )

		k = 1			k = 2		
		$u_c^d$	$\sigma_c$	$\sigma_c$	$u_c^d$	$\sigma_c$	$\sigma_c$
		numerical		analytical	numerical		analytical
$R_0/L_0 = 0.068$	deformation theory	6.109	1005.362	1005.387	6.177	1007.379	1007.285
	flow theory	6.109	1005.362	1005.393	6.203	1008.146	1007.373
$R_0/L_0 = 0.045$	deformation theory	6.096	1004.947	1005.036	6.130	1005.987	1005.879
	flow theory	6.098	1005.033	1005.044	6.133	1006.076	1005.896
$R_0/L_0 = 0.018$	deformation theory	6.089	1004.764	1004.799	6.096	1004.974	1004.934
	flow theory	6.089	1004.764	1004.800	6.096	1004.974	1004.938

**Figure 8.** Numerical and analytical values of  $u_c^d$  and  $\sigma_c$  at the two lowest bifurcations modes ( $n = 5$ )

		k = 1			k = 2		
		$u_c^d$	$\sigma_c$	$\sigma_c$	$u_c^d$	$\sigma_c$	$\sigma_c$
		numerical		analytical	numerical		analytical
$R_0/L_0 = 0.068$	deformation theory	2.905	591.751	591.754	2.948	592.578	592.508
	flow theory	2.908	591.809	591.794	2.984	593.262	593.150
$R_0/L_0 = 0.045$	deformation theory	2.899	591.634	591.615	2.917	591.983	591.950
	flow theory	2.899	591.634	591.623	2.923	592.098	592.077
$R_0/L_0 = 0.018$	deformation theory	2.893	591.518	591.521	2.899	591.635	591.574
	flow theory	2.893	591.518	591.521	2.899	591.635	591.574

**Figure 9.** Numerical and analytical values of  $u_c^d$  and  $\sigma_c$  at the two lowest bifurcations modes ( $n = 10$ )

**7. Conclusion**

In this paper we have established the analytical expression of the bifurcation stress of a cylinder under uniaxial tension when a  $J_2$  deformation theory is adopted. This expression shows that deformation theory predicts that bifurcation occurs sooner than the bifurcation predicted by the flow theory but both theories predict that bifurcation takes place after the maximum load point. We find here the same result as the one demonstrated by Hutchinson et Miles [HUT 74] and Needleman [NEE 72] for the flow theory: the more slender the cylinder, the closer the bifurcation is to the maximum. Our computations show that there is a very good agreement between analytical and finite element predictions.

## 8. References

- [BAT 49] BATDORF S. B., « Theories of plastic buckling ». *Journal of the aeronautical sciences*, 16, p. 405–408, 1949.
- [BUS 82] BUSHNELL D., « Theories of plastic buckling ».
- [CHE 71] CHENG S. Y., ARIARATNAM S. T. et DUBEY R. N. , « Axisymmetric bifurcation in an elastic-plastic cylinder under axial load and lateral hydrostatic pressure ». *Quarterly of applied mathematics*, p. 41–51, 1971.
- [HIL 58] HILL R., « A general theory of uniqueness and stability in elastic-plastic solids ». *Journal of the Mechanics and Physics of Solids*, 6, p. 236–249, 1958.
- [HUT 74] HUTCHINSON J. W. et MILES J. P. , « Bifurcation analysis of the onset of necking in an elastic/plastic cylinder under uniaxial tension ». *Journal of the Mechanics and Physics of Solids*, 22, p. 61–71, 1974.
- [MCM 75] MCMEEKING R. M. et RICE J. R. , « Finite-element formulations for problems of large elastic-plastic deformation ». *International Journal of Solids and Structures*, 11, p. 601–616, 1975.
- [MIL 71] MILES J. P., « Bifurcation in plastic flow under uniaxial tension ». *Journal of the Mechanics and Physics of Solids*, 19, p. 89–102, 1971.
- [NEE 72] NEEDLEMAN A., « A numerical study of necking in circular cylindrical bars ». *Journal of the Mechanics and Physics of Solids*, 20, p. 111–127, 1972.
- [NOR 78] NORRIS JR D. M., MORAN B., SCUDDER J. K. et QUINONES D. F., « A computer simulation of the tension test ». *Journal of the Mechanics and Physics of Solids*, 26, p. 1–19, 1978.
- [RUD 75] RUDNICKI J. W. et RICE J. R., « Conditions for the localization of deformation in pressure-sensitive dilatant materials ». *Journal of the Mechanics and Physics of Solids*, 23, p. 371–394, 1975.